

# Analysis of the August 2017 Eclipse's Effect on Radio Wave Propagation Employing a Raytrace Algorithm



M.L. Moses<sup>1</sup>, S. Burujupalli<sup>1</sup>, K. Brosie<sup>1</sup>, S. Dixit<sup>1</sup>, G.D. Earle<sup>1</sup>, L. Kordella<sup>1</sup>, N.A. Frissell<sup>2</sup>, C. Chitale<sup>1</sup>  
<sup>1</sup>Virginia Tech, <sup>2</sup>New Jersey Institute of Technology



## Introduction

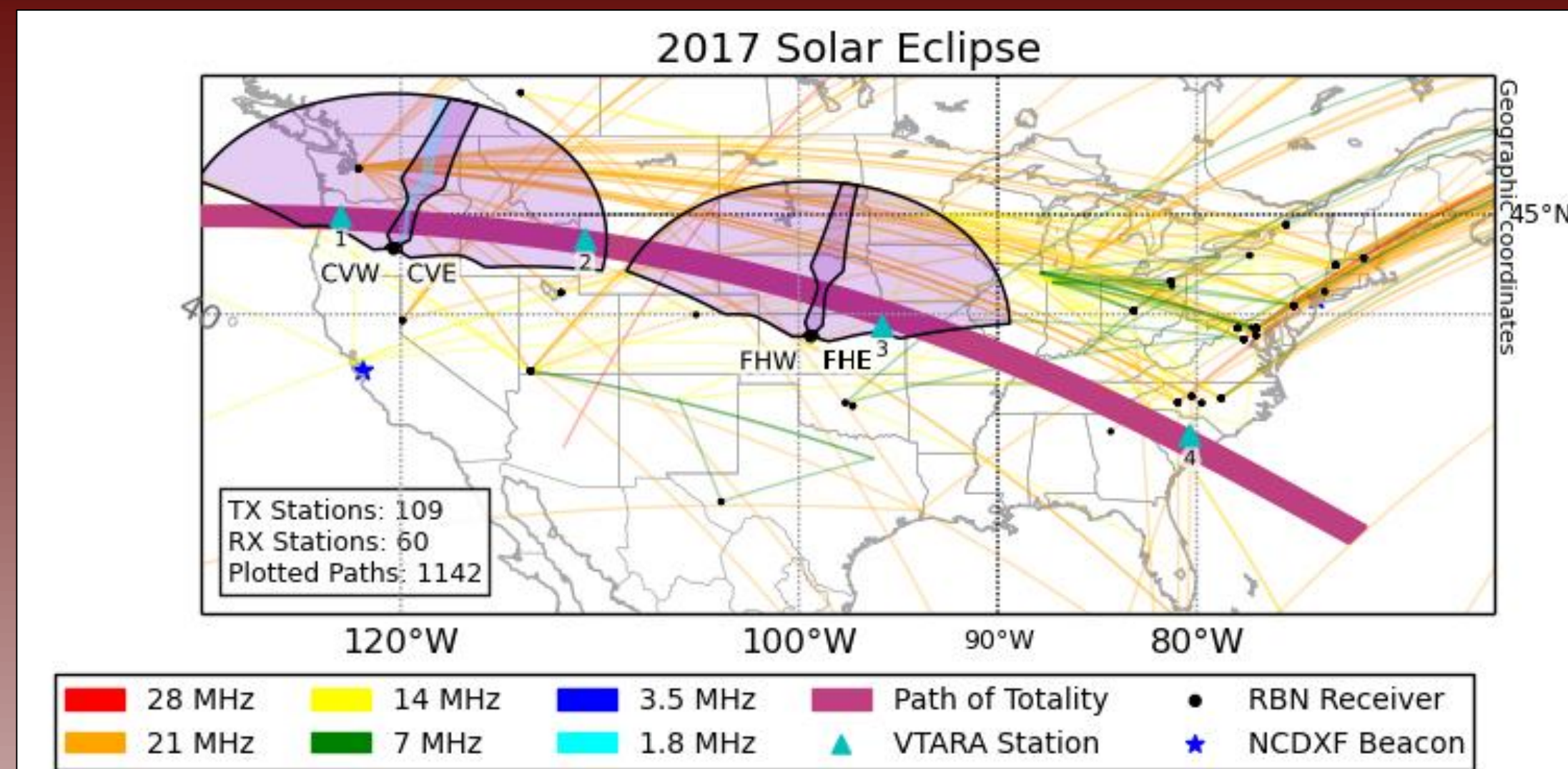


Figure 1. Eclipse path (maroon) will cross SuperDARN fields of view (violet) and affect ham radio propagation links (yellow, orange, and green).

The upcoming total solar eclipse over the continental United States on August 21 offers an unique opportunity to study the dependence of the ionospheric density and morphology on incident solar radiation. There are significant differences between the conditions during a solar eclipse and the conditions normally experienced at sunset and sunrise, including the west-to-east motion of the eclipse terminator, the duration of the event, the solar zenith angle, and the continued visibility of the corona. Taken together, these factors imply that unique ionospheric responses may be witnessed during eclipses, as measured by changes in radio frequency (RF) propagation. High Frequency (HF) propagation varies greatly depending on ionospheric conditions. Hence, our analysis will include data collected during the eclipse by several HF systems shown in Figure 1 including SuperDARN, temporary radio transceiver sites, and amateur radio networks such as the Reverse Beacon Network (RBN) and Weak Signal Propagation Reporter Network (WSPRNet). The data analysis will be guided by raytrace models of HF propagation through an eclipsed ionosphere employing the HF propagation toolbox, PHaRLAP (created by Dr. Manuel Cervera).

## Background

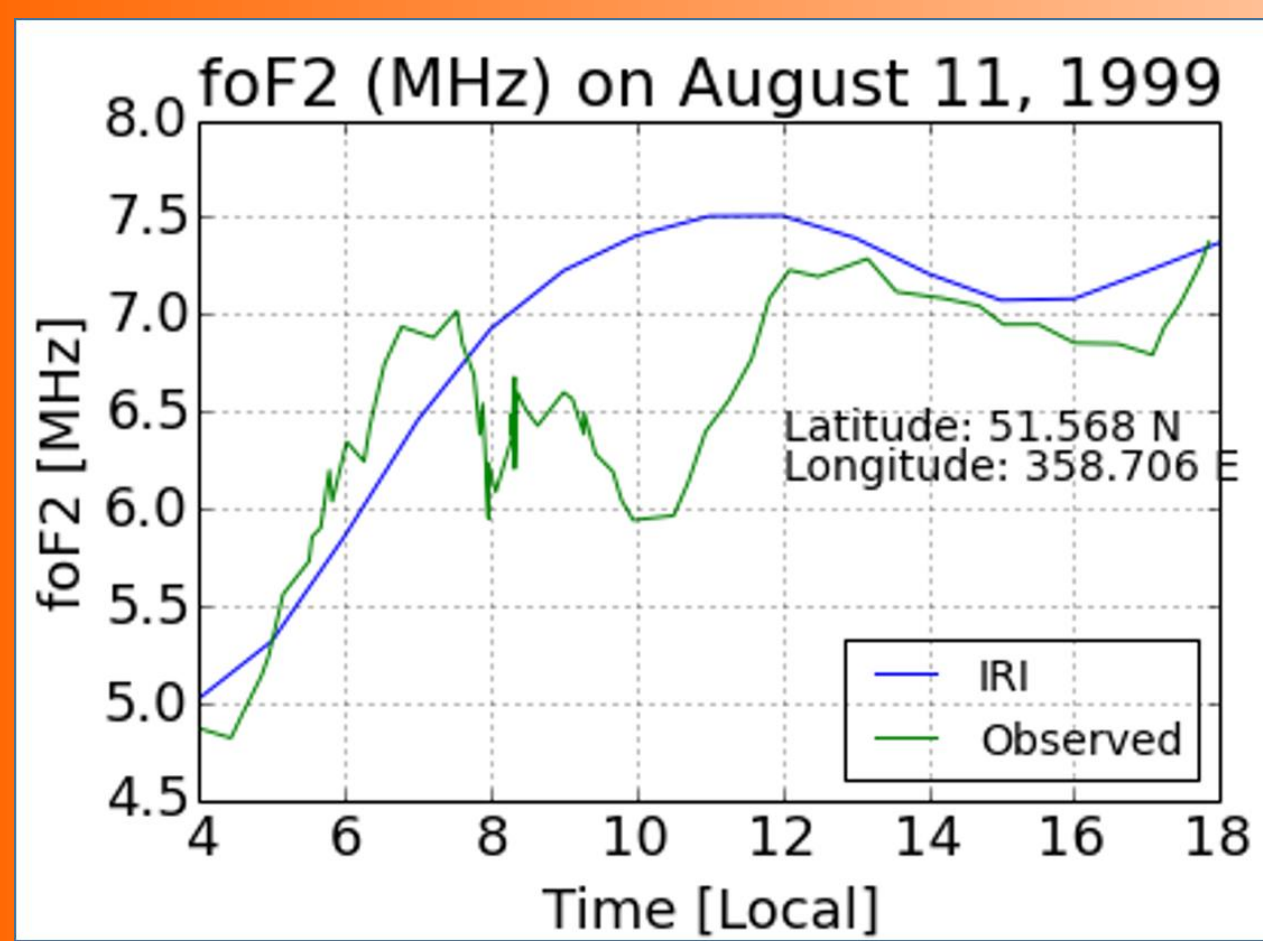


Figure 2. Effect of the August 11, 1999 eclipse on foF2 (Afraimovich et al., 2002)

- ❖ The Chilton ionosonde in Great Britain collected foF2 data during the August 1999 eclipse (Figure 2) that shows a distinct decrease in foF2 at the onset of the eclipse.
- ❖ The maximum deviation in foF2 from that date's IRI model is 20%. Hence, the electron density measured during the eclipse is about 64% of that predicted by the IRI for a normal day.

## Eclipse Attenuation Model

- ❖ A spline function matching the width and depth of the 1999 eclipse observations was created to model the attenuation.
- ❖ This model gave the fraction of eclipsed to uneclipsed electron density as a function of distance from the eclipse center at a given time.

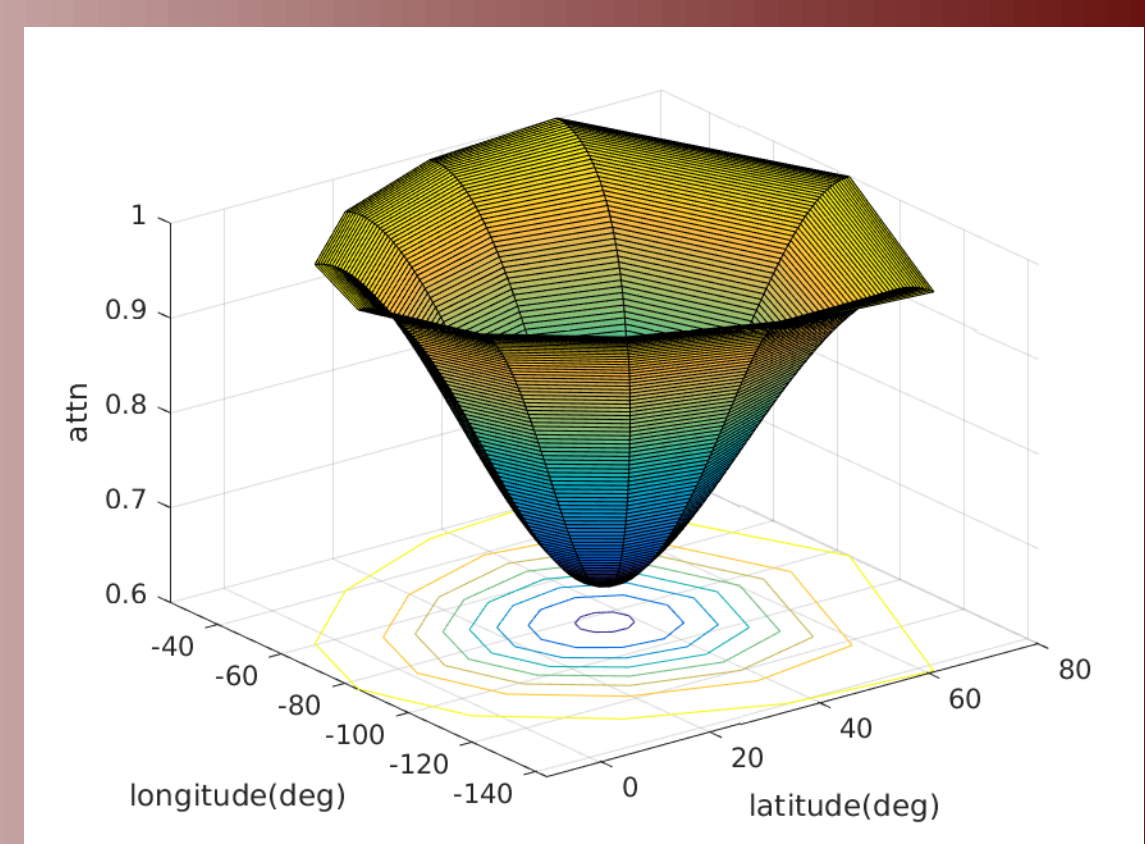


Figure 3. Attenuation as a Function of Distance from the Eclipse Center.

## Raytrace Algorithm

- ❖ Mapping of the attenuation function to three dimensions was accomplished by mapping the attenuation to coordinates of latitude and longitude centered at the point of maximum eclipse for a given time as shown in Figure 3.
- ❖ The attenuation factor was imposed on the IRI electron density expected for the eclipse date for all latitudes and longitudes independent of altitude.
- ❖ The PHaRLaP 3D raytracing code modeled propagation through this modified ionosphere as the eclipse progressed across the US.

## Results

### Side View

- ❖ As shown in Figure 4, ray paths incident on the eclipsed region are altered by the reduced plasma density associated with the eclipse.
- ❖ In general the rays refract at higher altitudes within the eclipsed region, as expected.

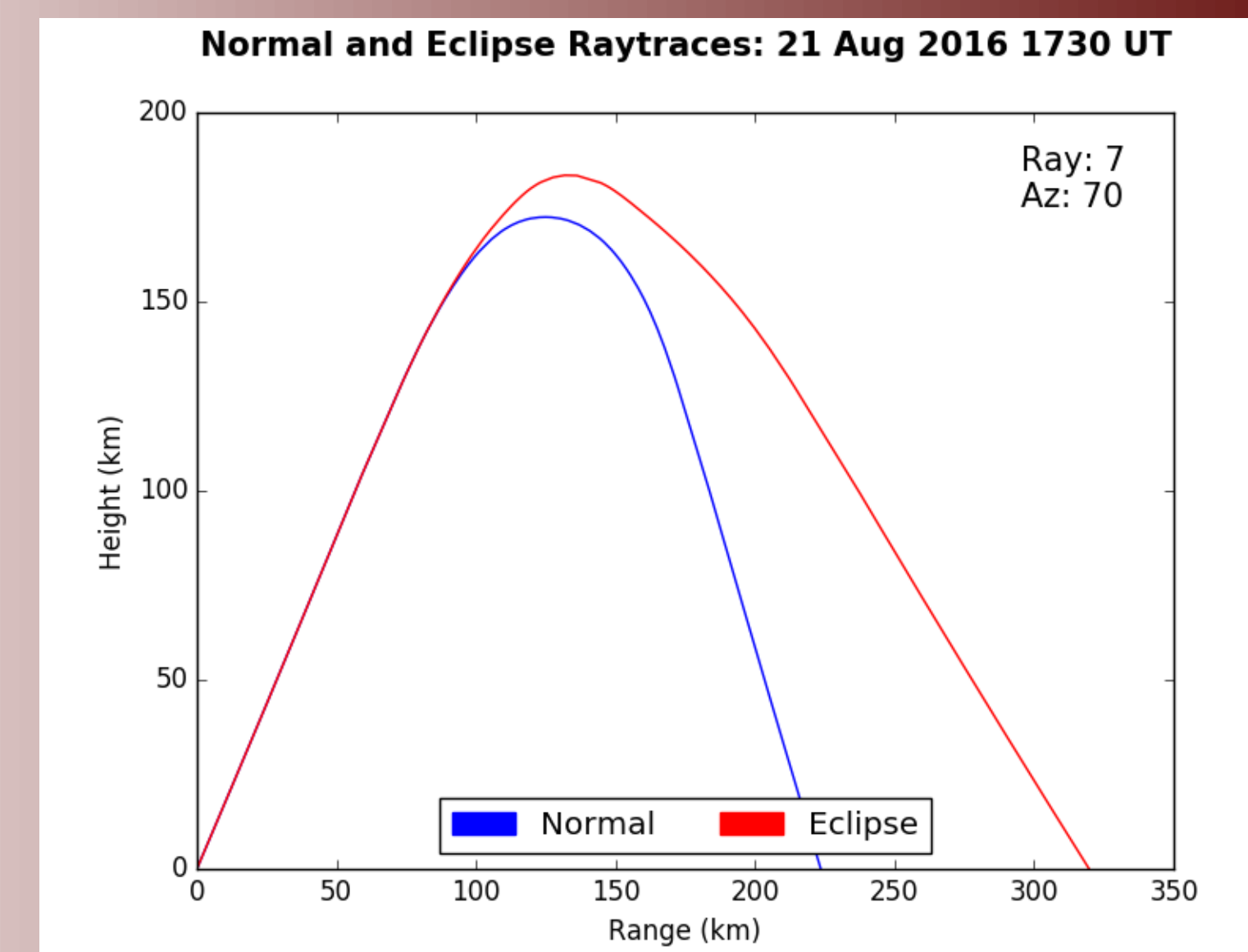


Figure 4. Ray-path of a 4 MHz beam at 60° elevation.

## Discussion

### Implication of Preliminary Results

- ❖ The data presented here indicate that the refractive effects of the eclipse change strongly with time as the eclipse progresses. The eclipsed raytrace model predicts ray-bending away from the modeled uneclipsed ray-path in both azimuth and elevation as well as changes in penetration depth and ground range. This has implications for how we interpret our HF datasets.

### Limitations of Current Model

- ❖ There are some limitations of this work due to certain assumptions made in our model for density across the eclipsed region such as the smooth and rotationally symmetric density decrease across the eclipse region. This is key factor that we hope to learn more about through our experiment.
- ❖ Refraction may be very different from what we predict due incorrect assumptions about the density in the umbra and penumbra stemming from transport mechanisms. For example, note the ionosonde data in Figure 2 shows that, although the plasma density recovers smoothly after the eclipse, the initial density decrease as the eclipse approaches totality is not monotonic. One hypothesis is that this behavior may be due to diffusion of plasma along the magnetic field lines from a higher altitude, uneclipsed region of the ionosphere. Effects like these will be studied with PHaRLaP and other simulation tools (e.g., SAMI-3) with constraints set by our observational data.

## Conclusions and Future Work

- ❖ The preliminary model predicts significant changes in RF propagation during the eclipse due to changes in the refractive index corresponding to the eclipse-induced ionospheric electron density attenuation.
- ❖ The results presented here demonstrate the utility of PHaRLaP to study HF ray propagation, which will aid in the post-eclipse data analysis.
- ❖ Further work leading up to the eclipse includes developing PHaRLaP – based tools to aid the post-eclipse SuperDARN, WSPRNet and RBN data analysis.
- ❖ After the eclipse, the data collected during the eclipse will be used to perform more detailed modeling in order to better understand the meso-scale physics of the F region during eclipses.

## References and Acknowledgments

E. L. Afraimovich, E. A. Kosogorov, and O. S. Lesyuta, "Effects of the August 11, 1999 total solar eclipse as deduced from total electron content measurements at the GPS network," *Journal of Atmospheric and Solar-Terrestrial Physics*, vol. 64, pp. 1933-1941, 12/2002

This work was supported by NSF Grant # AGS-1552188.

The results presented in this poster were obtained using the HF propagation toolbox, PHaRLaP, created by Dr. Manuel Cervera, Defence Science and Technology Organisation, Australia (manuel.cervera@dsto.defence.gov.au). This toolbox is available by request from its author.

We acknowledge the use of the Free Open Source Software projects used in this analysis: Ubuntu Linux, python, iPython, matplotlib, NumPy, SciPy, scikit-learn, DAVITpy, and others.

New Jersey Institute of Technology Eclipse Team (especially Joshua Vega and Joahua Katz).

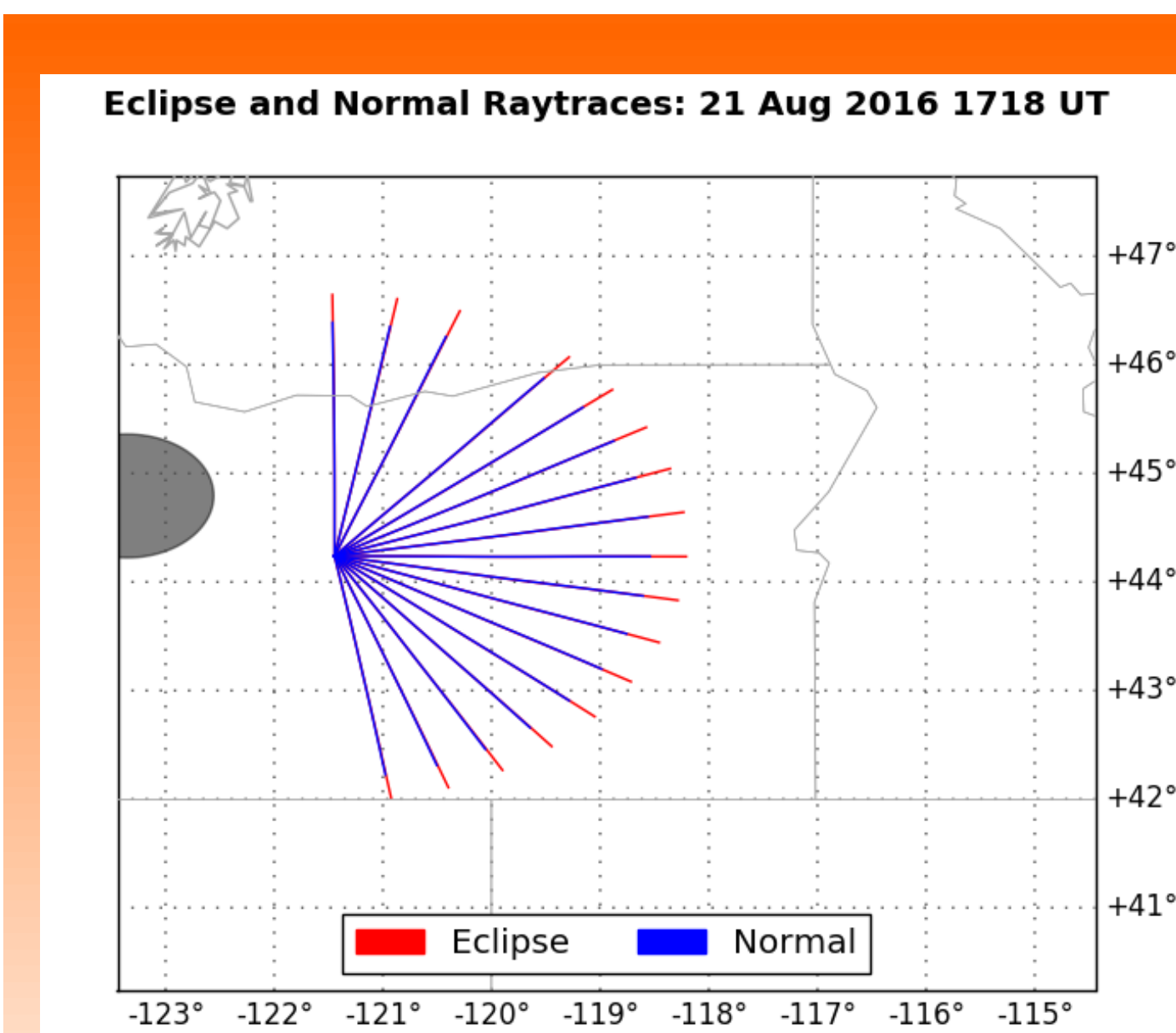


Figure 5a. Raytrace for transmitter at Site 1 in the penumbra before totality (the dark circle is the umbra boundary).

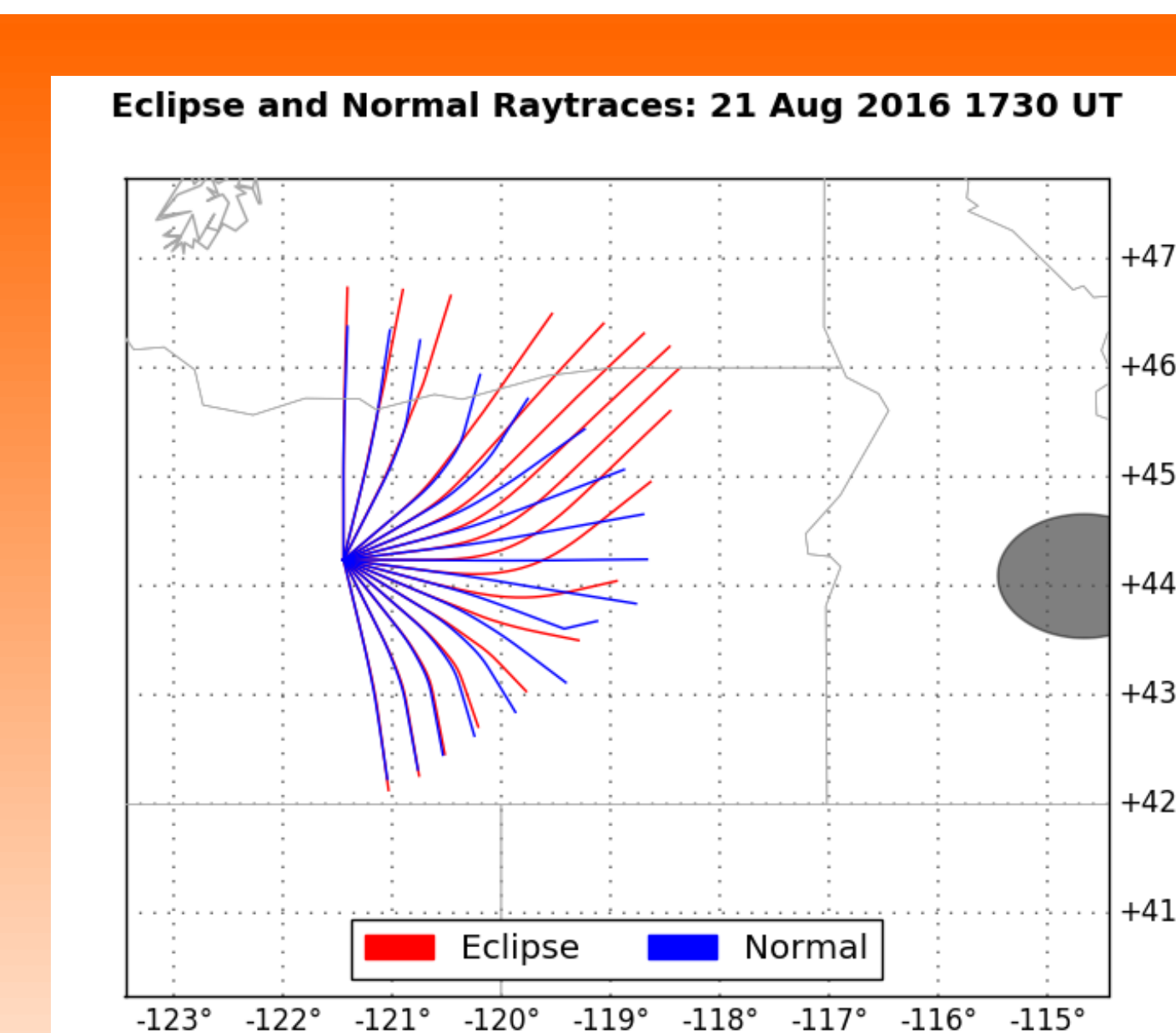


Figure 5b. Raytrace for the same beams traversing the penumbra after totality (the dark circle is the umbra boundary).

### Top View

- ❖ When the transmitter is in the penumbra before totality, ray paths calculated for rays directed parallel to the eclipse path appear to only experience a slight increase in path length as shown in Figure 5a. However, after the umbra has passed the transmitter, the rays are offset in azimuth from the paths they would have taken through an uneclipsed ionosphere as shown in Figure 5b. This suggests that the gradients in electron density produce a lensing effect at HF.